CLINICAL AND VACCINE IMMUNOLOGY, Feb. 2008, p. 227–234 Vol. 15, No. 2
1556-6811/08/$08.00+0 doi:10.1128/CVI.00334-07

Detection of *Mycobacterium avium* subsp. *paratuberculosis* by a Sonicate Immunoassay Based on Surface-Enhanced Raman Scattering[▽]

Betsy Jean Yakes,[1]† Robert J. Lipert,[1] John P. Bannantine,[2] and Marc D. Porter[1]*

Departments of Chemistry and Chemical and Biological Engineering, Ames Laboratory-USDOE, and Institute for Combinatorial Discovery, Iowa State University, Ames, Iowa 50011,[1] and USDA/ARS/National Animal Disease Center, Bacterial Diseases of Livestock Research Unit, Ames, Iowa 50010[2]

Received 13 August 2007/Returned for modification 5 September 2007/Accepted 2 November 2007

A sandwich immunoassay for the rapid, low-level detection of *Mycobacterium avium* subsp. *paratuberculosis* has been developed. *M. avium* subsp. *paratuberculosis* is the causative agent of Johne's disease in cattle, and one of the major obstacles in controlling the spread of this disease is the inability to rapidly detect small amounts of bacteria or other diagnostic markers shed during the subclinical stage of infection. This paper details the development and performance of an assay for sonicated *M. avium* subsp. *paratuberculosis* lysate that is based on surface-enhanced Raman scattering (SERS). There are two key components of the assay: (i) an immobilized layer of monoclonal antibodies that target a surface protein on the microorganism; and (ii) extrinsic Raman labels (ERLs) that are designed to selectively bind to captured proteins and produce large SERS signals. By correlating the number of *M. avium* subsp. *paratuberculosis* bacilli present prior to sonication to the amount of total protein in the resulting sonicate, the detection limit determined for total protein can be translated to the microorganism concentration. These findings yield detection limits of 100 and 200 ng/ml (estimated to be 500 and 1,000 *M. avium* subsp. *paratuberculosis* bacilli/ml) for sonicate spiked in phosphate buffer and sonicate spiked in whole milk, respectively. Moreover, the time required to complete the assay, which includes sample preparation, antigen extraction, ERL incubation, and readout, is less than 24 h. The potential for incorporation of this novel assay into diagnostic laboratories is also briefly discussed.

Johne's disease is responsible for devastating losses in worldwide dairy production (54). The causative agent of this disease is *Mycobacterium avium* subsp. *paratuberculosis*. *M. avium* subsp. *paratuberculosis* has been found in domestic ruminants (39, 44, 55, 56) and wildlife (6–8, 23, 28, 34, 41, 42, 66). Based on a serological survey conducted by the National Animal Health Monitoring System in 1996 and 2002 (27, 61), 20 to 40% of the cattle herds in the United States are afflicted with *M. avium* subsp. *paratuberculosis* at some level. Moreover, the 1996 National Animal Health Monitoring System report and an economic loss study by Ott and coworkers projected that the annual economic impact on the U.S. dairy industry from this disease exceeds 200 million dollars annually (27, 46).

Cattle are often exposed to *M. avium* subsp. *paratuberculosis* as calves (58). The disease develops through four stages and is generally diagnosed by symptomatic assessment and, when possible, quantification of shed bacteria. The four stages of progression are silent, subclinical, clinical, and advanced cellular infection (65). During the silent stage, animals do not shed detectable amounts of the bacteria and are asymptomatic. In the subclinical phase, cattle shed small amounts of *M. avium* subsp. *paratuberculosis* in their feces and milk (e.g., 10 CFU per 50 ml of milk) (30) but still at levels that are difficult to rapidly and reliably detect. Nevertheless, this subtle shedding can contaminate the surrounding habitat and spread *M. avium* subsp. *paratuberculosis* throughout a herd before its presence is detected. In the clinical phase of infection, the pathogen is shed at high levels, which can exceed 10^{10} organisms/g of feces (11). Symptoms during the terminal, advanced cellular infection stage of the disease are exemplified by chronic diarrhea, rapid weight loss, diffuse edema, reduced milk production, and infertility.

There is a wide range of tests for *M. avium* subsp. *paratuberculosis*. Bacteriologic culture is the most accepted method and benefits from readily available materials. When coupled with symptomatic evaluation, culturing provides data central to distinguishing between clinical and subclinical stages of Johne's disease. Culturing, however, typically requires 12 to 16 weeks of incubation (see the Johne's Information Center website at http://johnes.vetmed.wisc.edu/). Serological tests, including complement fixation, agar gel immunodiffusion, and enzyme-linked immunosorbent assay, reduce testing time but can lack the sensitivity needed to detect *M. avium* subsp. *paratuberculosis* at subclinical levels (12–14, 16, 52, 53, 65). Methods that test for cellular immunity, such as the response to delayed-type hypersensitivity and detection of elevated levels of gamma interferon (IFN-γ), can yield false-positive reactions (32). Nucleic acid levels, after PCR amplification and analysis by gel electrophoresis, can be determined in under 3 days (Johne's Information Center) and can detect 10 *M. avium* subsp. *paratuberculosis* bacilli in a 2-ml milk sample when immunomagnetic concentration is used (36). However, there are challenges related to specificity (15, 24) and performance in

* Corresponding author. Present address: Department of Chemistry, University of Utah, Salt Lake City, UT 84108. Phone: (801) 587-1505. Fax: (801) 585-0575. E-mail: marc.porter@utah.edu.

† Present address: U.S. FDA-CFSAN, 5100 Paint Branch Parkway, College Park, MD 20740.

▽ Published ahead of print on 12 December 2007.

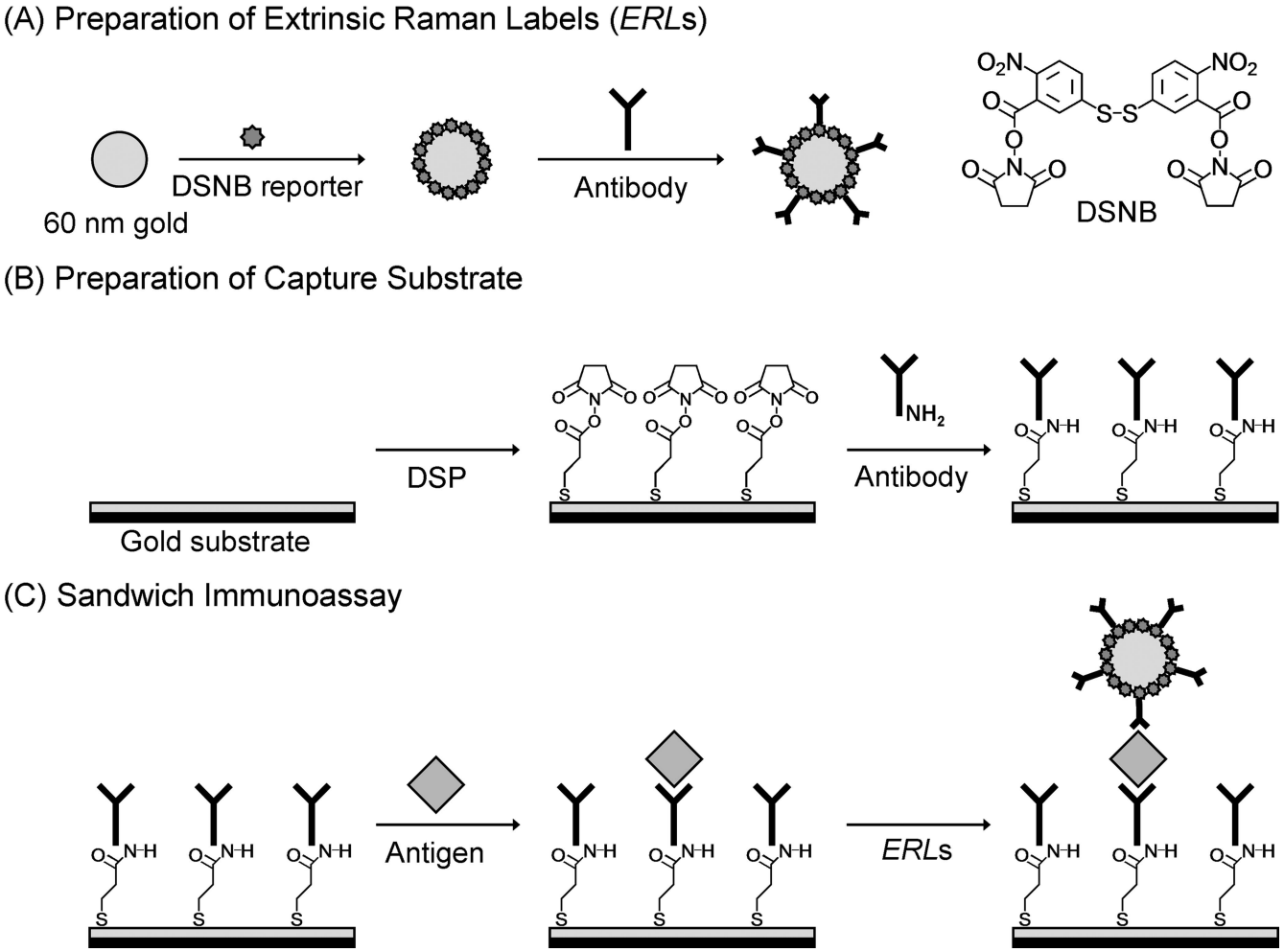

FIG. 1. Schematic of the substrate preparation and assay procedure for the SERS readout sandwich immunoassay. (A) SERS tracer formation. (B) Capture substrate preparation. (C) Antigen extraction and labeling.

some complex sample matrices (36). It is therefore clear that improvements in sensitivity, selectivity, sample workup, speed, and detection are requisite to more effectively protect healthy animals against infection and the subsequent development and spread of Johne's disease (10).

This work explores the potential of surface-enhanced Raman scattering (SERS) to serve as a readout method for the detection of *M. avium* subsp. *paratuberculosis* at low levels. Several laboratories, including our own, have demonstrated the merits of SERS readout in immunoassays (1, 19, 20, 31, 43, 45, 47, 51, 67, 69) and DNA detection (9, 25, 29). In SERS, roughened metal surfaces amplify the Raman scattering of an adsorbed organic molecule. This enhancement is due mainly to increases in the electromagnetic field at the nanometric asperities of roughened coinage metals (e.g., silver and gold). The same mechanism is operative at the surface of metallic nanoparticles. Coupled with potential contributions from chemical effects, enhancements of up to 10^{14} have been reported (37).

Detection by SERS has several potentially valuable attributes with respect to traditional signal transduction methods such as radioisotope decay, colorimetry, and fluorescence (26, 40, 45). First, when employing gold nanoparticles, excitation in the red spectral region is used, which minimizes possible interference from native fluorescence. Second, SERS intensities for immobilized molecules are beginning to approach those of fluorescent dyes and have the added feature of being less susceptible to photobleaching. Finally, the widths of Raman spectral bands are typically 10 to 100 times narrower than those of fluorescence, which reduces the potential for spectral overlap from multiple labels. The work herein seeks to take advantage of the first two attributes for the development of a rapid and highly sensitive assay for *M. avium* subsp. *paratuberculosis*.

The SERS-based strategy uses extrinsic Raman labels (ERLs) as a means to quantitatively take advantage of amplified scattering (20–22, 31, 45, 47–50). ERLs (Fig. 1A) incorporate the intrinsically strong Raman scattering of aromatic compounds (i.e., reporter molecules). In this assay, the organic molecule is first immobilized on the gold nanoparticles and is then used to tether a molecular recognition element (e.g., an antibody) to the surface. The preparation of the capture substrate (Fig. 1B) employs the same chemistry, with the coupling molecule forming a gold-bound thiolate and subsequently reacting with the primary amines on antibodies. We note that the

depictions in Fig. 1 are idealized with respect to the positions of the immobilized antibodies. A more random distribution of orientations is expected because of the presence of amine residues throughout the structure of the protein (18). Finally, a sandwich immunoassay (Fig. 1C) can be carried out in less than 24 h by (i) extracting the antigen from solution, (ii) labeling the captured antigen with ERLs, and (iii) quantitating the tagged antigen by SERS. We have previously applied this platform to the detection of immunoglobulin G (45), free prostate-specific antigen (31), viruses (20), and simulants of biological warfare agents (47). Those works showed that the SERS-based immunoassay not only offers low levels of detection (e.g., ~30 fM for prostate-specific antigen in human serum) but is also sufficiently sensitive to measure single binding events (49).

This paper and the companion paper (68) explore the adaptation and performance of a highly sensitive SERS-based immunoassay system as a specific and rapid diagnostic platform for Johne's disease. As a first step, the activity and cross-reactivity of a group of recently developed antibodies that selectively target proteins located at the outer surface of *M. avium* subsp. *paratuberculosis* cells (2) were evaluated. After incorporating the most effective antibody onto both the capture substrate and the ERLs, assays for the detection of K-10 *M. avium* subsp. *paratuberculosis* sonicate were carried out. By estimating the number of *M. avium* subsp. *paratuberculosis* bacilli present prior to sonication with the amount of total protein in sonicate solution, detection limits of approximately 500 and 1,000 *M. avium* subsp. *paratuberculosis* cells/ml for sonicate spiked in phosphate buffer and in whole milk, respectively, were achieved. The companion paper extends this optimized system to the detection of whole-cell *M. avium* subsp. *paratuberculosis* and investigates the possibility of signal amplification (68).

MATERIALS AND METHODS

Bacteria and sonicate preparation. Heat-killed, whole-cell *M. avium* subsp. *paratuberculosis* (K-10 bovine isolate) cells were grown at 37°C in Middlebrook 7H9 medium (Becton Dickinson, Cockeysville, MD) that was supplemented with 2 mg of mycobactin J/liter (Allied Monitor Inc., Fayette, MO), 10% oleic acid albumin–dextrose complex (Becton Dickinson), and 0.05% Tween 80 (Sigma-Aldrich, St. Louis, MO). The bacilli, harvested from the culture medium by centrifugation at 10,000 × *g* for 20 min, were washed twice with cold phosphate-buffered saline solution (PBS) (0.15 M, pH 7.2). Following washing, the bacteria were either heat treated (80°C for 30 min) or sonicated.

Whole-cell sonicated extracts of *M. avium* subsp. *paratuberculosis* cells in PBS (pH 7.4) were produced as described previously (64). After culturing *M. avium* subsp. *paratuberculosis* cells to an optical density at 540 nm of 0.2 to 0.4 and centrifuging the cells, the pellet was resuspended in PBS and sonicated. Sonication used a probe sonicator and consisted of three 10-min cycles at 18 W on ice, with 10-min chilling periods between each sonication. Debris was removed by centrifugation (12,000 × *g* for 5 min), and supernatants were harvested and stored at 20°C.

Stock solution concentrations of heat-killed, whole-cell bacteria were determined by (i) flow cytometry using a Live/Dead Bac*Light* bacterial viability and counting kit (Molecular Probes, Eugene, OR), (ii) bacterial enumeration through serial dilution plating on Herrold's egg yolk slants containing mycobactin J (2 mg/liter), and/or (iii) measurements of the optical density at 540 nm. The average value for the stock solutions used in immunoassay development was $1.3 \pm 0.3 \times 10^7$ bacteria/ml (six samples of *M. avium* subsp. *paratuberculosis* in PBS). The bacterial concentration for the stock solution used for sonication was 5×10^6 *M. avium* subsp. *paratuberculosis* cells/ml. After sonication, the solution had a total protein concentration of 1 mg/ml based on absorbance measurements at 280 nm with an ND-1000 spectrophotometer (NanoDrop Technologies, Inc., Rockland, DE). This value was further confirmed by using the Bio-Rad protein assay (Richmond, CA).

Heat-killed *Salmonella enterica* serovar Typhimurium and heat-killed *Escherichia coli* O157:H7 were gifts from Nancy Cornick (Department of Veterinary Microbiology and Preventive Medicine, Iowa State University, Ames).

Sonicate spiked samples in PBS and whole milk. Antigen solutions were prepared by serial dilution of the stock K-10 sonicate with 10 mM PBS (pH 7.4) (10 mM PBS powder packs; Sigma-Aldrich) or pasteurized, whole milk. Between dilutions, solutions were mixed by vortexing. Distilled water, subsequently deionized with a Millipore (Billerica, MA) Milli-Q system (18 MΩ), was used for the preparation of all aqueous reagents. For assays in a milk matrix, whole milk at room temperature was employed in place of PBS during serial dilution. Specifically, the first dilutions were prepared by adding 10 μl of 1 mg/ml sonicate in PBS to either 10 μl of whole milk or 90 μl of whole milk; all subsequent dilutions used whole milk.

Antibodies. Monoclonal antibodies (mAbs) to MAP2121c, an *M. avium* subsp. *paratuberculosis* surface protein, have recently been produced (4). Three monoclonal antibodies (8G2, 13E1, and 12C9, with the former two being specific for the MAP2121c protein) were tested for performance after purification using Melon gel (Pierce, Rockford, IL). This step removes extraneous proteins that could potentially compete with immobilization of the mAb from the tissue culture supernatants. The concentrations of the mAb solutions were determined spectrophotometrically (ND-1000, using a standard mass extinction coefficient of 13.7 liters g^{-1} cm^{-1} for 10 mg/ml immunoglobulin G solution as a reference); all mAb dilutions employed 50 mM borate buffer (pH 8.3 borate buffer packs; Pierce).

ERL preparation. The design, preparation, and optimization of the ERLs were detailed in our previous work (20). Briefly, 1.0 ml of 60-nm gold particles (<8% variation in diameter, 2.6×10^{10} particles/ml; Ted Pella, Redding, CA) was added to a centrifuge vial. The pH of the suspension was adjusted with 40 μl of 50 mM borate buffer (pH 8.3). Ten microliters of 1.4 mM DSNB [5,5′-dithiobis(succinimidyl-2-nitrobenzoate)] in acetonitrile (high-performance liquid chromatography grade; Fisher, Pittsburgh, PA) was added to this colloidal suspension. DSNB was synthesized according to previously described methods, and it coats the gold nanoparticles through chemisorption as the corresponding thiolate (59, 70). After 7 h, 20 μg of one of the three mAbs was added to the mixture and incubated for ~14 h. At pH 8.3, the amines on the mAb are deprotonated and can therefore form amide linkages upon a reaction with the succinimidyl esters of the DSNB-based monolayer (33). Finally, to block unreacted succinimidyl esters, as well as to stabilize the colloidal suspension, 100 μl of 10% bovine serum albumin (BSA) (Sigma-Aldrich) in 2 mM borate buffer was added to the suspension and allowed to react for 7 h.

Next, the colloidal suspension was centrifuged (MiniSpin; Eppendorf, Westbury, NY) at 2,000 × *g* for 10 min at room temperature to remove excess reagents. After decanting the clear supernatant, the loose colloidal gold pellet was resuspended in 1,000 μl of 2 mM borate buffer containing 1% BSA. This centrifugation-resuspension procedure was repeated twice to maximize the removal of excess reagent. The volume after the last resuspension step was 500 μl. Finally, 50 μl of 10% sodium chloride (Sigma-Aldrich) was added to the suspension, which was then passed through a Costar 0.22-μm syringe filter (Fisher) to remove any aggregates.

Capture surface preparation. The fabrication of the capture substrate was done according to procedures described previously (20, 31, 45, 47). Template-stripped gold was prepared by resistively evaporating ~300 nm of gold (99.9%) at 0.1 to 0.2 nm/s onto a 4-in. P-type test-grade silicon [111] wafer (University Wafer, South Boston, MA) using an Edwards 306A evaporator. After applying cleaned 1- by 1-cm glass chips onto the gold surface via two-part epoxy (Epo-tek 377) and oven curing at 150°C for 1.75 h, the glass slides were carefully separated from the wafer, exposing a smooth gold surface.

A poly(dimethyl siloxane) (Dow Corning, Midland, MI) stamp with a centered, 3.2-mm-diameter hole was soaked in a 2 mM ethanolic solution of octadecanethiol (Sigma-Aldrich). The stamp was dried under a stream of high-purity nitrogen and used to ink the template-stripped gold substrate for ~30 s. This procedure formed a hydrophobic barrier that surrounded the 3.2-mm assay address (38). These samples were subsequently exposed to a 0.1 mM ethanolic (Aaper, Shelbyville, KY) solution of dithiobis(succinimidyl propionate) (DSP) (Sigma-Aldrich) for ~14 h, which formed a DSP-derived monolayer within the address area. After rinsing with ethanol and drying under a stream of nitrogen, 20 μl of capture antibody (100 μg/ml) was dispensed onto each substrate. This step couples the antibody to the DSP-based monolayer by the same mechanism as that used for DSNB. After incubation for 7 h in a humidity chamber, the substrates were rinsed three times with 2 ml of 10 mM PBS buffer. Unreacted succinimidyl end groups of the monolayer were "capped" with a 20-μl drop of

blocking buffer for ~14 h (i.e., SuperBlock and StarterBlock [Pierce], 5% BSA in PBS, 2% Carnation dry milk in PBS, or casein blocking solution [Sigma-Aldrich]).

Immunoassay procedure. After blocking, the capture surface was exposed to either a solution of heat-killed, whole-cell *M. avium* subsp. *paratuberculosis* cells or concentrations of K-10 sonicate in 10 mM PBS (pH 7.4) for 7 h at room temperature in a humidity chamber. After rinsing three times with 2 mM borate buffer (pH 8.3) (150 mM NaCl), a 20-μl drop of the ERLs was placed onto the substrates and allowed to react for ~14 h. The substrates were again washed with the 2 mM borate solution and gently dried with nitrogen, and the SERS spectra were collected. This procedure followed that depicted in Fig. 1C.

SERS measurements: NanoRaman I spectrometer. Raman spectra were collected using a NanoRaman I spectrometer (Concurrent Analytical, Waimanalo, HI). This instrument consists of an HeNe laser (632.8 nm, 30 mW), a fiber optic-based probe head, an *f*/2.0 Czerny-Turner imaging spectrometer (6- to 8-cm^{-1} resolution), and a thermoelectrically cooled charge-coupled device (0°C) (Kodak 0401E). The laser light was focused as a 25-μm spot (2 to 3 mW) onto the substrate at normal incidence via an objective with a numerical aperture of 0.68, which also collected the scattered radiation. Exposure times of 1 s were employed, with an average of four or five measurements, as noted in Results, collected from different locations on each sample.

RESULTS

Antibody screening. As shown in work on feline calicivirus (K. M. Kwarta, J. D. Driskell, M. D. Porter, J. D. Neill, and J. F. Ridpath, unpublished data), candidate antibodies should be screened to determine those that are the most effective at binding the antigen after immobilization on the capture substrate (35). As such, dot blot reactivity with heat-killed, whole-cell *M. avium* subsp. *paratuberculosis* was used to narrow a pool of eight mAbs, which were selected from an ongoing Johne's Disease Integrated Program project (4, 5), to three mAbs. These three mAbs were designated 13E1, 12C9, and 8G2. Both 13E1 and 8G2 react with different epitopes on MAP2121c (4), and 12C9 binds to an unidentified *M. avium* subsp. *paratuberculosis* protein (5). After purification, each antibody was tested by performing an immunoassay with an antigen concentration of 1.0×10^7 *M. avium* subsp. *paratuberculosis* cells/ml and a PBS blank.

Using the sensor platform depicted in Fig. 1, the SERS spectra shown in Fig. 2 were obtained. The strongest feature in each spectrum (1,336 cm^{-1}) is assigned to a symmetric nitro stretch [$\nu_s(NO_2)$], while the less intense band (1,588 cm^{-1}) is diagnostic of an aromatic ring mode. These and all the other spectral features present are consistent with those expected for the DSNB-derived monolayer. Furthermore, the evolution of the intensities of these features is indicative of the amount of ERLs and thus antigen bound to the surface; that is, a larger SERS signal is diagnostic of a higher level of captured antigen. The intensity for $\nu_s(NO_2)$ in each assay, as obtained from measurements at four locations per sample, was 293 ± 75 counts/s for 8G2, 223 ± 80 counts/s for 12C9, and 1,611 ± 63 counts/s for 13E1. The blank, shown only for 13E1, had a signal of 256 ± 21 counts/s. Based on 13E1 having the largest SERS intensity and approximately the same blank signal as those for 12C9 and 8G2 substrates exposed to *M. avium* subsp. *paratuberculosis*, 13E1 was the most effective of the mAbs for the SERS substrate.

These samples were also examined by light microscopy. The images showed that only 13E1 substrates captured an observable amount of *M. avium* subsp. *paratuberculosis*, which is roughly a 1.5- by 0.5-μm rod. In contrast, the substrates coated with 12C9 or 8G2 exhibited little evidence of binding (data not shown). Based on the combined weight of these two sets of results, 13E1 was chosen for the remainder of the studies. It is important to note that while 12C9 and 8G2 mAbs had higher titers and stronger immunoblot responses (J. P. Bannantine, unpublished data), 13E1 was more effective when immobilized on the capture substrate. This finding exemplifies the importance of screening mAbs after being tethered to substrates in a heterogeneous immunoassay (17; Kwarta et al., unpublished).

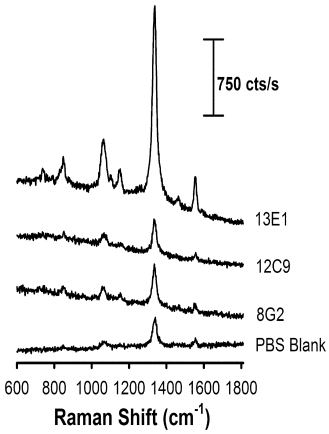

FIG. 2. Representative SERS spectra in screening studies using the heterogeneous immunoassay (vertically offset for clarity) for mAbs 8G2, 12C9, and 13E1 reacted with 1.0×10^7 heat-killed *M. avium* subsp. *paratuberculosis* cells/ml and a PBS blank with 13E1. Data show that 13E1 had the highest $\nu_s(NO_2)$ intensity in counts per second (cts/s). The blank spectrum for 13E1 is comparable to those for 12C9 and 8G2.

Antibody specificity assessment. Cross-reactivity is another important figure of merit for diagnostic methods. Specificity studies of 13E1 with other closely related mycobacteria have recently been performed via immunoblots (4). Those studies revealed that 13E1 also reacted with *Mycobacterium avium* complex members. However, and more importantly, there was a lack of detectable cross-reactivity with *Mycobacterium bovis*, the other mycobacterial pathogen in cattle, as well as with non-*Mycobacterium avium* complex mycobacteria potentially present in bovine feces or milk.

To further assess specificity, cross-reactivity studies were performed on immobilized 13E1 with two commonly occurring bacteria in bovine milk and feces: *E. coli* O157:H7 (60) and *S. enterica* serovar Typhimurium (62, 63). After exposing the samples to a single type of bacterium and then ERLs, the intensity for $\nu_s(NO_2)$ was obtained. As shown in Fig. 3, the results yielded 231 ± 16 counts/s for the PBS blank (no bacteria), 279 ± 23 counts/s for 1.0×10^8 CFU of *E. coli* O157:H7/ml, and 135 ± 15 counts/s for 7.3×10^9 cells of *S. enterica* serovar Typhimurium/ml. While more exhaustive cross-reactivity studies remain to be performed, specifically with *M. bovis* and other mycobacteria, these results indicate that there is no loss in selectively when 13E1 is immobilized on the capture substrate.

Blocking reagent evaluation. As part of an optimization protocol, studies to determine which blocking agent would minimize the blank signal while maximizing the response to *M. avium* subsp. *paratuberculosis* were performed. To this end, solutions of SuperBlock, StartingBlock, 5% BSA in PBS, 2% dry milk in PBS, casein-based blocker, or PBS (no blocker)

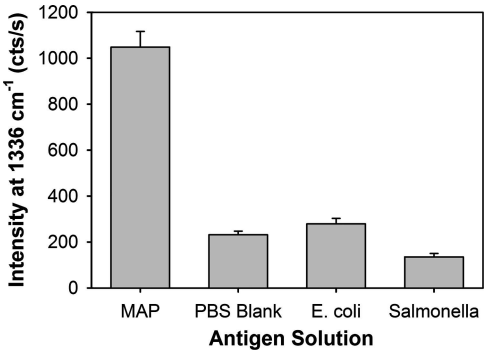

FIG. 3. 13E1 cross-reactivity with commonly occurring bacteria in bovine feces. Each substrate was exposed to 1.0×10^5 *M. avium* subsp. *paratuberculosis* (MAP) cells/ml, a PBS blank, *E. coli* O157:H7 (1.0×10^8 CFU/ml), or *Salmonella* (7.3×10^9 cells/ml). 13E1 did not cross-react with *E. coli* or *Salmonella*, as signals were comparable to those of the PBS blank.

were placed onto separate 13E1 substrates. These substrates were then exposed to PBS (blank) or to a solution containing 1.0×10^5 *M. avium* subsp. *paratuberculosis* cells/ml. The results from the SERS readout of each sample are summarized in Fig. 4. The samples treated with StartingBlock had the highest signal for *M. avium* subsp. *paratuberculosis* but, according to the blank response, also had the highest level of nonspecific adsorption of ERLs. Moreover, the blocking solutions of 5% BSA, 2% dry milk, and casein failed to remain confined in the 3.2-mm sample address because of their low surface tension. This "drop spreading" led to low signals for the *M. avium* subsp. *paratuberculosis*-containing samples. While PBS (no blocker) and SuperBlock have roughly the same blank and *M. avium* subsp. *paratuberculosis* signals, the precision of the measurement was three times better for SuperBlock. Based on these results, SuperBlock was used in subsequent studies.

K-10 sonicate in PBS assay. The K-10 sonicate samples, with concentrations ranging from 1×10^2 to 5×10^5 ng/ml, were incubated with the capture platform (Fig. 1B). After rinsing, the substrates were exposed to ERLs (Fig. 1C). Importantly, these two steps, as well as those involved in sample preparation

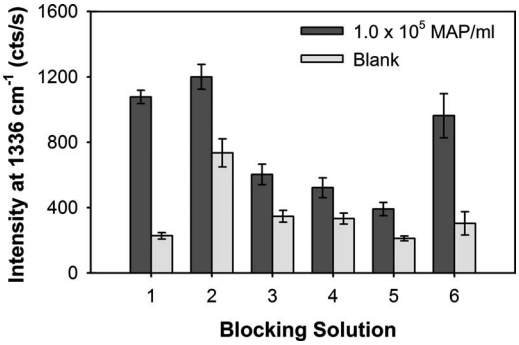

FIG. 4. SERS intensity for ERLs binding to *M. avium* subsp. *paratuberculosis* (MAP) after blocking with SuperBlock (1), StartingBlock (2), 5% bovine serum albumin in PBS (3), 2% dry milk in PBS (4), casein-based blocker (5), or PBS/no blocker (6) and either a PBS blank or 1.0×10^5 *M. avium* subsp. *paratuberculosis*/ml for the antigen step. SuperBlock yielded the largest SERS intensity and lowest blank signal. cts/s, counts per second.

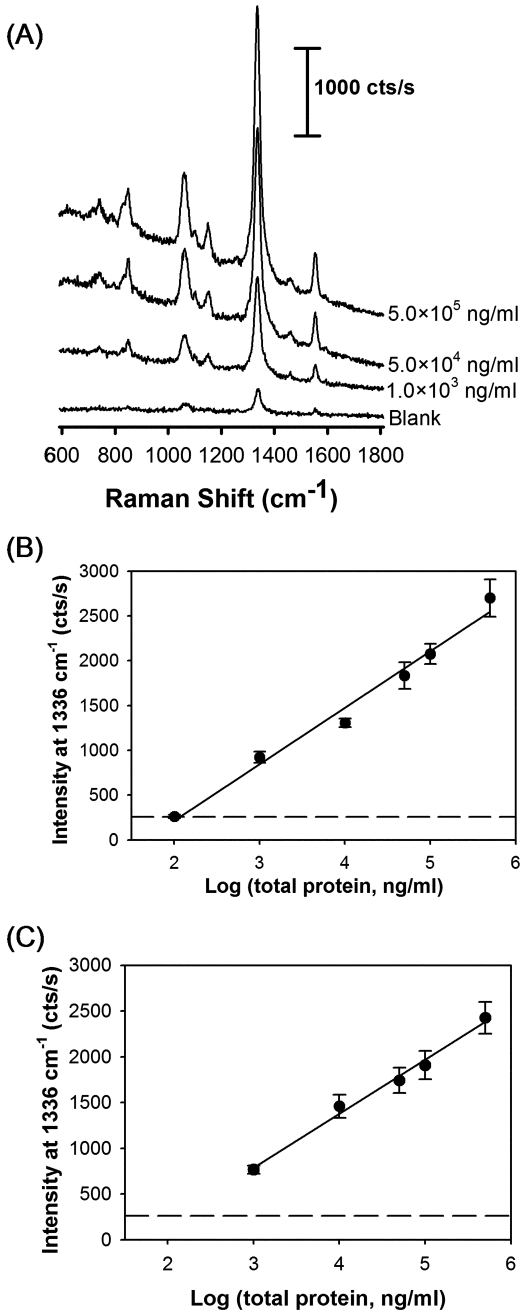

FIG. 5. Spectra and calibration curve for sonicate-spiked PBS and milk samples. (A) Spectra (vertically offset for clarity) for sonicate in PBS. (B) Corresponding calibration curve from SERS measurements. (C) Calibration curve for sonicate in milk. Dashed lines correspond to the blank plus three times its standard deviation for each matrix. Best-fit lines are as follows: $y = 631x - 1{,}048$ ($R^2 = 0.98$) (B) and $y = 592x - 993$ ($R^2 = 0.99$) (C).

(e.g., sonication), require less than 24 h to complete. The resulting SERS spectra were collected with a 1-s read time, and the calibration curve was prepared by subtracting the background at 1,225 cm^{-1} from the intensity of $\nu_s(NO_2)$ at 1,336 cm^{-1}. Both data sets are given in Fig. 5A and B. As is evident, the SERS signals increased in a concentration-dependent manner with sonicated antigen. The lowest detectable signal, as

defined by the blank signal plus three times its standard deviation, is indicated by the dashed line in the calibration curve. The limit of detection (LOD), which corresponds to the intersection of these two curves, was calculated to be ~100 ng/ml. Since the original solution (5×10^6 *M. avium* subsp. *paratuberculosis* cells/ml) produced 1 mg/ml of total protein after sonication and centrifugation, the LOD for the K-10 sonicate in terms of whole cells is estimated to be ~500 *M. avium* subsp. *paratuberculosis* cells/ml. This estimation is based on two criteria. First, when correlating the number of bacilli to sonicate protein, it is expected that the levels of newly synthesized proteins in the cytoplasm are negligible compared to those already transported to the surface. In addition, as there is some insoluble protein (debris) that is removed following centrifugation of the sonicate, the conversion to bacilli/ml is an approximation.

K-10 sonicate in milk assay. To determine the feasibility of analyzing relevant biological samples, an initial study was performed using a milk matrix. Room temperature, pasteurized, whole milk was spiked with the K-10 sonicate for concentrations up to 5×10^5 ng/ml. As described above, the assay procedure was performed in fewer than 24 h, with the resulting calibration curve shown in Fig. 5C. Importantly, the milk matrix plot is strongly similar to that of the PBS matrix in Fig. 5B; that is, the close agreement between the best-fit lines (i.e., slopes and *y* intercepts) and precision (i.e., standard deviations for individual samples) indicate that the performance achieved in the clean PBS matrix is not compromised when using the much more complex matrix of whole milk. Furthermore, the plot in Fig. 5C translates to an LOD of ~200 ng/ml (estimated at ~1,000 *M. avium* subsp. *paratuberculosis* bacilli/ml). These findings begin to elucidate the robust nature of this assay system with respect to its potential application in complex matrices. These results also demonstrate that analysis in whole milk can be carried out with little sample workup.

DISCUSSION

There is a wide range of diagnostic tests for Johne's disease, each with previously detailed strengths and limitations in performance. To protect healthy animals from this disease and minimize its spread, more effective means to identify infected cattle, track disease development, and further characterize each of the clinical stages are necessary. The results herein demonstrate that the SERS-based immunoassay can potentially address these objectives. LODs for the K-10 sonicate are ~100 ng/ml (~500 *M. avium* subsp. *paratuberculosis* cells/ml) in PBS and ~200 ng/ml (~1,000 *M. avium* subsp. *paratuberculosis* cells/ml) in pasteurized, whole milk. This level of performance, realized in less than 24 h, is a direct result of the integration of the 13E1 antibody as a recognition element with SERS as a readout tool.

There are several features of this assay that translate to advantages over other techniques. First, IFN-γ detection, as an indirect method, can be problematic because of false-positive results. PCR, while a direct method, may yield false-negative results in complex matrices (57). Immunoassay techniques, including enzyme-linked immunosorbent assay and this SERS-based immunoassay, improve detection over IFN-γ detection and PCR by incorporating antibody recognition. In this system, the 13E1 mAb targets a surface protein (MAP2121c) that plays a role in the *M. avium* subsp. *paratuberculosis* invasion of epithelial cells (3). The screening and cross-reactivity studies carried out previously (4) and in this work highlight the specificity of this mAb, which may yield a lower number of false-positive results in clinical samples. Of particular importance is the lack of detectable cross-reactivity with *M. bovis*, which is the other mycobacterial pathogen found in cattle.

Second, the assay takes advantage of recent developments that have transformed SERS into a powerful analytical tool. Of particular importance is the emergence of nanoparticles as SERS surfaces. In this system, the spontaneous adsorption of sulfur compounds to gold (59, 70) allows an adlayer of DSNB-based label to coat the nanoparticle surface. In addition, the DSNB-derived monolayer can tether antibodies and thus form a biospecific label. By incorporating these ERLs into a sandwich immunoassay, the *M. avium* subsp. *paratuberculosis* concentration is quantified by the intensity of the intrinsically strong $\nu_s(NO_2)$ of the DSNB-derived monolayer, and low-levels of detection are obtained. In addition, the good precision/reproducibility in measurements seen in the sonicate immunoassay is partially due to recent advances in the formation of uniform nanoparticles and preparation of optimized ERLs.

Another important feature of the SERS-based assay is its potential for integration into diagnostic laboratories. The instrumentation (a fiber optic-based Raman spectrometer) has no moving parts, is easy to use, and has a small footprint on the laboratory benchtop. In addition, breakthroughs in optical filters and detectors have decreased the costs of key hardware, with instrument pricing from several manufacturers on the order of $10,000 to $15,000. Moreover, other components of the assay can be readily packaged into a kit that includes both premade capture substrates and ERLs. Based on this, an assay would be performed by capturing the antigen from milk and incubating ERLs in under 24 h, and research to extend the assay to fecal samples is in progress.

In summary, we believe that this novel assay is well positioned to address many of the challenges associated with Johne's disease detection, especially with respect to speed, specificity, and sensitivity. To further accomplish these goals, experiments focusing on analyzing samples from animals clinically infected with *M. avium* subsp. *paratuberculosis*, extending the assay to fecal matter, and comparing the results of these samples with those for other established detection techniques are under way. Ongoing work is also aimed at improving performance by examining approaches to reduce nonspecific adsorption, thus improving the limit of detection, through rotating capture substrates and designing better assay surfaces. In addition, studies to further amplify the SERS signal from ERLs (e.g., stronger Raman scatterers and shape-tailored nanoparticles) are being undertaken. These improvements have the potential to allow the detection of tens of *M. avium* subsp. *paratuberculosis* cells/ml, thus allowing the SERS-based immunosensor to be applicable to subclinical samples. Finally, the potential extension of this assay to the detection of whole *M. avium* subsp. *paratuberculosis* bacteria is detailed in the companion paper (68).

ACKNOWLEDGMENTS

We acknowledge Jeremy Driskell for helpful conversations.

This work was supported by the Institute for Combinatorial Discovery of Iowa State University and by a grant through the CEROS/DARPA. The Ames Laboratory is operated for the U.S. Department of Energy by Iowa State University under contract no. DE-AC02-07CH11358. We also acknowledge support from the USDA-NRI-CAP Johne's Disease Integrated Program to J.P.B. as well as support from the USDA's Agricultural Research Service.

REFERENCES

1. **Ansari, D. O., D. A. Stuart, and S. Nie.** 2005. Surface-enhanced Raman spectroscopic detection of cancer biomarkers in intact cellular specimens. Proc. SPIE **5699:**82–90.
2. **Bannantine, J. P., E. Baechler, Q. Zhang, L. Li, and V. Kapur.** 2002. Genome scale comparison of *Mycobacterium avium* subsp. *paratuberculosis* with *Mycobacterium avium* subsp. *avium* reveals potential diagnostic sequences. J. Clin. Microbiol. **40:**1303–1310.
3. **Bannantine, J. P., J. F. Huntley, E. Miltner, J. R. Stabel, and L. E. Bermudez.** 2003. The Mycobacterium avium subsp. paratuberculosis 35 kDa protein plays a role in invasion of bovine epithelial cells. Microbiology **149:**2061–2069.
4. **Bannantine, J. P., T. J. Radosevich, J. R. Stabel, S. Berger, J. F. Griffin, and M. L. Paustian.** 2007. Production and characterization of monoclonal antibodies against a major membrane protein of *Mycobacterium avium* subsp. *paratuberculosis*. Clin. Vaccine Immunol. **14:**312–317.
5. **Bannantine, J. P., T. J. Radosevich, J. R. Stabel, S. Sreevatsan, V. Kapur, and M. L. Paustian.** 2007. Development and characterization of monoclonal antibodies and aptamers against major antigens of *Mycobacterium avium* subsp. *paratuberculosis*. Clin. Vaccine Immunol. **14:**518–526.
6. **Beard, P. M., M. J. Daniels, D. Henderson, A. Pirie, K. Rudge, D. Buxton, S. Rhind, A. Greig, M. R. Hutchings, I. McKendrick, K. Stevenson, and J. M. Sharp.** 2001. Paratuberculosis infection of nonruminant wildlife in Scotland. J. Clin. Microbiol. **39:**1517–1521.
7. **Beard, P. M., S. M. Rhind, D. Buxton, M. J. Daniels, D. Henderson, A. Pirie, K. Rudge, A. Greig, M. R. Hutchings, K. Stevenson, and J. M. Sharp.** 2001. Natural paratuberculosis infection in rabbits in Scotland. J. Comp. Pathol. **124:**290–299.
8. **Burton, M. S., J. H. Olsen, R. L. Ball, and G. A. Dumonceaux.** 2001. Mycobacterium avium subsp. paratuberculosis infection in an addax (Addax nasomaculatus). J. Zoo Wildl. Med. **32:**242–244.
9. **Cao, Y. C., R. Jin, and C. A. Mirkin.** 2002. Nanoparticles with Raman spectroscopic fingerprints for DNA and RNA detection. Science **297:**1536–1540.
10. **Chacon, O., L. E. Bermudez, and R. G. Barletta.** 2004. Johne's disease, inflammatory bowel disease, and Mycobacterium paratuberculosis. Annu. Rev. Microbiol. **58:**329–363.
11. **Chiodini, R. J., H. J. Van Kruiningen, and R. S. Merkal.** 1984. Ruminant paratuberculosis (Johne's disease): the current status and future prospects. Cornell Vet. **74:**218–262.
12. **Clarke, C. J., I. A. Patterson, K. E. Armstrong, and J. C. Low.** 1996. Comparison of the absorbed ELISA and agar gel immunodiffusion test with clinicopathological findings in ovine clinical paratuberculosis. Vet. Rec. **139:**618–621.
13. **Colgrove, G. S., C. O. Thoen, B. O. Blackburn, and C. D. Murphy.** 1989. Paratuberculosis in cattle: a comparison of three serologic tests with results of fecal culture. Vet. Microbiol. **19:**183–187.
14. **Collins, M. T., S. J. Wells, K. R. Petrini, J. E. Collins, R. D. Schultz, and R. H. Whitlock.** 2005. Evaluation of five antibody detection tests for diagnosis of bovine paratuberculosis. Clin. Diagn. Lab. Immunol. **12:**685–692.
15. **Cousins, D. V., R. Whittington, I. Marsh, A. Masters, R. J. Evans, and P. Kluver.** 1999. Mycobacteria distinct from Mycobacterium avium subsp. paratuberculosis isolated from the feces of ruminants possess IS900-like sequences detectable by IS900 polymerase chain reaction: implications for diagnosis. Mol. Cell. Probes **14:**431–442.
16. **Dargatz, D. A., B. A. Byrum, L. K. Barber, R. W. Sweeney, R. H. Whitlock, W. P. Shulaw, R. H. Jacobson, and J. R. Stabel.** 2001. Evaluation of a commercial ELISA for diagnosis of paratuberculosis in cattle. J. Am. Vet. Med. Assoc. **218:**1163–1166.
17. **Diamandis, E. P., and T. K. Christopoulos (ed.).** 1996. Immunoassay. Academic Press, San Diego, CA.
18. **Dong, Y., and C. Shannon.** 2000. Heterogeneous immunosensing using antigen and antibody monolayers on gold surfaces with electrochemical and scanning probe detection. Anal. Chem. **72:**2371–2376.
19. **Dou, X., T. Takama, Y. Yamaguchi, and H. Yamamoto.** 1997. Enzyme immunoassay utilizing surface-enhanced Raman scattering of the enzyme reaction product. Anal. Chem. **69:**1492–1495.
20. **Driskell, J. D., K. M. Kwarta, R. J. Lipert, M. D. Porter, J. D. Neill, and J. F. Ridpath.** 2005. Low-level detection of viral pathogens by a surface-enhanced Raman scattering based immunoassay. Anal. Chem. **77:**6147–6154.
21. **Driskell, J. D., R. J. Lipert, and M. D. Porter.** 2006. Labeled gold nanoparticles immobilized at smooth metallic substrates: systematic investigation of surface plasmon resonance and surface-enhanced Raman scattering. J. Phys. Chem. B **110:**17444–17451.
22. **Driskell, J. D., J. M. Uhlenkamp, R. J. Lipert, and M. D. Porter.** 2007. Surface-enhanced Raman scattering immunoassays using a rotated capture substrate. Anal. Chem. **79:**4141–4148.
23. **Dukes, T. W., G. J. Glover, B. W. Brooks, J. R. Duncan, and M. Swendrowski.** 1992. Paratuberculosis in saiga antelope (Saiga tatarica) and experimental transmission to domestic sheep. J. Wildl. Dis. **28:**161–170.
24. **Ellingson, J. L. E., J. R. Stabel, W. R. Bishai, R. Frothingham, and J. M. Miller.** 2000. Evaluation of the accuracy and reproducibility of a practical PCR panel assay for rapid detection and differentiation of Mycobacterium avium subspecies. Mol. Cell. Probes **14:**153–161.
25. **Faulds, K., W. E. Smith, and D. Graham.** 2005. DNA detection by surface enhanced resonance Raman scattering (SERRS). Analyst **130:**1125–1131.
26. **Garrell, R. L.** 1989. Surface-enhanced Raman spectroscopy. Anal. Chem. **61:**401A–402A, 404A, 406A–408A, 410A–411A.
27. **Garry, F. S. Wells, S. Ott, and D. Hansen.** 1999. Animal and Plant Health Inspection Service info sheet: who can afford a $200 loss per cow? Or Johne's disease—what do I need to know, p. 1–7. http://www.aphis.usda.gov/vs/ceah/ncahs/nahms/dairy/dairy96/johnsart.htm.
28. **Godfroid, J., C. Delcorps, L. M. Irenge, K. Walravens, S. Marche, and J. L. Gala.** 2005. Definitive differentiation between single and mixed mycobacterial infections in red deer (Cervus elaphus) by a combination of duplex amplification of p34 and f57 sequences and Hpy188I enzymatic restriction of duplex amplicons. J. Clin. Microbiol. **43:**4640–4648.
29. **Graham, D., B. J. Mallinder, D. Whitcombe, N. D. Watson, and W. E. Smith.** 2002. Simple multiplex genotyping by surface-enhanced resonance Raman scattering. Anal. Chem. **74:**1069–1074.
30. **Grant, I. R., H. J. Ball, and M. T. Rowe.** 2002. Incidence of *Mycobacterium paratuberculosis* in bulk raw and commercially pasteurized cows' milk from approved dairy processing establishments in the United Kingdom. Appl. Environ. Microbiol. **68:**2428–2435.
31. **Grubisha, D. S., R. J. Lipert, H. Y. Park, J. Driskell, and M. D. Porter.** 2003. Femtomolar detection of prostate-specific antigen: an immunoassay based on surface-enhanced Raman scattering and immunogold labels. Anal. Chem. **75:**5936–5943.
32. **Harris, N. B., and R. G. Barletta.** 2001. *Mycobacterium avium* subsp. *paratuberculosis* in veterinary medicine. Clin. Microbiol. Rev. **14:**489–512.
33. **Hermanson, G. T.** 1996. Bioconjugate techniques. Academic Press, San Diego, CA.
34. **Judge, J., I. Kyriazakis, A. Greig, D. J. Allcroft, and M. R. Hutchings.** 2005. Clustering of *Mycobacterium avium* subsp. *paratuberculosis* in rabbits and the environment: how hot is a hot spot? Appl. Environ. Microbiol. **71:**6033–6038.
35. **Kenseth, J. R., K. M. Kwarta, J. D. Driskell, M. D. Porter, J. D. Neill, and J. F. Ridpath.** 2007. Strategies in the use of atomic force microscopy as a multiplexed readout tool of chip-scale protein motifs, p. 81–107. *In* S. Mallapragada and B. Narasimhan (ed.), Combinatorial materials science. John Wiley and Sons, Hoboken, NJ.
36. **Khare, S., T. A. Ficht, R. L. Santos, J. Romano, A. R. Ficht, S. Zhang, I. R. Grant, M. Libal, D. Hunter, and L. G. Adams.** 2004. Rapid and sensitive detection of *Mycobacterium avium* subsp. *paratuberculosis* in bovine milk and feces by a combination of immunomagnetic bead separation-conventional PCR and real-time PCR. J. Clin. Microbiol. **42:**1075–1081.
37. **Kneipp, K., H. Kneipp, I. Itzkan, R. R. Dasari, and M. S. Feld.** 2002. Surface-enhanced Raman scattering and biophysics. J. Phys. Condens. Matter **14:**R597–R624.
38. **Kumar, A., and G. M. Whitesides.** 1993. Features of gold having micrometer to centimeter dimensions can be formed through a combination of stamping with an elastomeric stamp and an alkanethiol "ink" followed by chemical etching. Appl. Phys. Lett. **63:**2002–2004.
39. **Lambeth, C., L. A. Reddacliff, P. Windsor, K. A. Abbott, H. McGregor, and R. J. Whittington.** 2004. Intrauterine and transmammary transmission of Mycobacterium avium subsp. paratuberculosis in sheep. Aust. Vet. J. **82:**504–508.
40. **Long, D.** 2002. The Raman effect. Wiley, New York, NY.
41. **Machackova-Kopecna, M., M. Bartos, M. Straka, V. Ludvik, P. Svastova, J. Alvarez, J. Lamka, I. Trcka, F. Treml, I. Parmova, and I. Pavlik.** 2005. Paratuberculosis and avian tuberculosis infections in one red deer farm studied by IS900 and IS901 RFLP analysis. Vet. Microbiol. **105:**261–268.
42. **Mackintosh, C. G., G. W. de Lisle, D. M. Collins, and J. F. Griffin.** 2004. Mycobacterial diseases of deer. N. Z. Vet. J. **52:**163–174.
43. **Mulvaney, S. P., M. D. Musick, C. D. Keating, and M. J. Natan.** 2003. Glass-coated, analyte-tagged nanoparticles: a new tagging system based on detection with surface-enhanced Raman scattering. Langmuir **19:**4784–4790.
44. **Muskens, J., D. Bakker, J. de Boer, and L. van Keulen.** 2001. Paratuberculosis in sheep: its possible role in the epidemiology of paratuberculosis in cattle. Vet. Microbiol. **78:**101–109.
45. **Ni, J., R. J. Lipert, G. B. Dawson, and M. D. Porter.** 1999. Immunoassay readout method using extrinsic Raman labels adsorbed on immunogold colloids. Anal. Chem. **71:**4903–4908.
46. **Ott, S. L., S. J. Wells, and B. A. Wagner.** 1999. Herd-level economic losses associated with Johne's disease on US dairy operations. Prev. Vet. Med. **40:**179–192.
47. **Park, H.-Y.** 2005. Chip-scale bioassays based on surface-enhanced Raman

scattering: fundamentals and applications. Ph.D. thesis. Iowa State University, Ames.
48. **Park, H.-Y., J. D. Driskell, K. M. Kwarta, R. J. Lipert, M. D. Porter, C. Schoen, J. D. Neill, and J. F. Ridpath.** 2006. Ultrasensitive immunoassays based on surface-enhanced Raman scattering by immunogold labels. Top. Appl. Phys. **103:**427–446.
49. **Park, H.-Y., R. J. Lipert, and M. D. Porter.** 2004. Single particle Raman measurements of gold nanoparticles used in surface-enhanced Raman scattering (SERS)-based sandwich immunoassays. Proc. SPIE **5593:**464.
50. **Porter, M. D., J. D. Driskell, K. M. Kwarta, R. J. Lipert, J. D. Neill, and J. F. Ridpath.** 2006. Detection of viruses: atomic force microscopy and surface enhanced Raman spectroscopy. Dev. Biol. **126:**31–39.
51. **Rohr, T. E., T. Cotton, N. Fan, and P. J. Tarcha.** 1989. Immunoassay employing surface-enhanced Raman spectroscopy. Anal. Biochem. **182:**388–398.
52. **Sergeant, E. S., R. J. Whittington, and S. J. More.** 2002. Sensitivity and specificity of pooled fecal culture and serology as flock-screening tests for detection of ovine paratuberculosis in Australia. Prev. Vet. Med. **52:**199–211.
53. **Sockett, D. C., T. A. Conrad, C. B. Thomas, and M. T. Collins.** 1992. Evaluation of four serological tests for bovine paratuberculosis. J. Clin. Microbiol. **30:**1134–1139.
54. **Stabel, J. R.** 1998. Johne's disease: a hidden threat. J. Dairy Sci. **81:**283–288.
55. **Storset, A. K., I. Berg, and B. Djonne.** 2005. Evaluation of the gamma interferon test for diagnosis of paratuberculosis in goats. Vet. Immunol. Immunopathol. **107:**87–94.
56. **Storset, A. K., H. J. Hasvold, M. Valheim, H. Brun-Hansen, G. Berntsen, S. K. Whist, B. Djonne, C. M. Press, G. Holstad, and H. J. Larsen.** 2001. Subclinical paratuberculosis in goats following experimental infection. An immunological and microbiological study. Vet. Immunol. Immunopathol. **80:**271–287.
57. **Stratmann, J., B. Strommenger, K. Stevenson, and G.-F. Gerlach.** 2002. Development of a peptide-mediated capture PCR for detection of *Mycobacterium avium* subsp. *paratuberculosis* in milk. J. Clin. Microbiol. **40:**4244–4250.
58. **Sweeney, R. W.** 1996. Transmission of paratuberculosis. Vet. Clin. N. Am. Food Anim. Pract. **12:**305–312.
59. **Ulman, A.** 1996. Formation and structure of self-assembled monolayers. Chem. Rev. **96:**1533–1554.
60. **USDA.** 2003. Animal and Plant Health Inspection Service info sheet: Escherichia coli O157 on U.S. dairy operations, p. 1-3. http://www.aphis.usda.gov/vs/ceah/ncahs/nahms/dairy/dairy02/Dairy02Ecoli.pdf.
61. **USDA.** 2005. Animal and Plant Health Inspection Service info sheet: highlights of NAHMS Johne's disease on U.S. dairy operations, 2002, p. 1-4. http://www.aphis.usda.gov/vs/ceah/ncahs/nahms/dairy/dairy02/Dairy02_Johnes_highlights.pdf.
62. **USDA.** 2003. Animal and Plant Health Inspection Service info sheet: Salmonella and Campylobacter on U.S. dairy operations, p. 1-3. http://www.aphis.usda.gov/vs/ceah/ncahs/nahms/dairy/dairy02/Dairy02SalCampy.pdf.
63. **USDA.** 2005. Animal and Plant Health Inspection Service info sheet: Salmonella on U.S. dairy operations; prevalence and antimicrobial drug susceptibility, p. 1–4. http://www.aphis.usda.gov/vs/ceah/ncahs/nahms/dairy/dairy02/Dairy02_Salmonella.pdf.
64. **Waters, W. R., J. M. Miller, M. V. Palmer, J. R. Stabel, D. E. Jones, K. A. Koistinen, E. M. Steadham, M. J. Hamilton, W. C. Davis, and J. P. Bannantine.** 2003. Early induction of humoral and cellular immune responses during experimental *Mycobacterium avium* subsp. *paratuberculosis* infection of calves. Infect. Immun. **71:**5130–5138.
65. **Whitlock, R. H., S. J. Wells, R. W. Sweeney, and J. Van Tiem.** 2000. ELISA and fecal culture for paratuberculosis (Johne's disease): sensitivity and specificity of each method. Vet. Microbiol. **77:**387–398.
66. **Whittington, R. J., I. B. Marsh, and R. H. Whitlock.** 2001. Typing of IS 1311 polymorphisms confirms that bison (Bison bison) with paratuberculosis in Montana are infected with a strain of Mycobacterium avium subsp. paratuberculosis distinct from that occurring in cattle and other domesticated livestock. Mol. Cell. Probes **15:**139–145.
67. **Xu, S., X. Ji, W. Xu, X. Li, L. Wang, Y. Bai, B. Zhao, and Y. Ozaki.** 2004. Immunoassay using probe-labelling immunogold nanoparticles with silver staining enhancement via surface-enhanced Raman scattering. Analyst **129:**63–68.
68. **Yakes, B. J., R. J. Lipert, J. P. Bannantine, and M. D. Porter.** 2008. Impact of protein shedding on detection of *Mycobacterium avium* subsp. *paratuberculosis* by a whole-cell immunoassay incorporating surface-enhanced Raman scattering. Clin. Vaccine Immunol. **15:**235–242.
69. **Zhang, X., M. A. Young, O. Lyandres, and R. P. Van Duyne.** 2005. Rapid detection of an anthrax biomarker by surface-enhanced Raman spectroscopy. J. Am. Chem. Soc. **127:**4484–4489.
70. **Zhong, C. J., and M. D. Porter.** 1995. Designing interfaces at the molecular level. Anal. Chem. **67:**709A–717A.